Available online at www.sciencedirect.com
ScienceDirect
Colloids and Surfaces A: Physicochem. Eng. Aspects 318 (2008) 78–83
COLLOIDS AND SURFACES A
www.elsevier.com/locate/colsurfa

On the aggregation phenomena of Au nanoparticles: Effect of substrate roughness on the particle size

Ahmad M. Mohammad [a,b], Ahmed I. Abdelrahman [a], Mohamed S. El-Deab [a,b], Takeyoshi Okajima [a], Takeo Ohsaka [a,*]

[a] *Department of Electronic Chemistry, Interdisciplinary Graduate School of Science and Engineering, Tokyo Institute of Technology, Mail Box G 1-5, 4259 Nagatsuta, Midori-ku, Yokohama 226-8502, Japan*
[b] *Chemistry Department, Faculty of Science, Cairo University, Cairo, Egypt*

Received 14 August 2007; received in revised form 3 December 2007; accepted 7 December 2007
Available online 22 January 2008

Abstract

A monolayer of chemically prepared gold nanoparticles (AuNPs, with an initial average particle size of 2.3 nm) was immobilized on three Au substrates with different roughness. 1,4-Benzenedimethanethiol (BDMT) was used as the immobilizing binder to connect the AuNPs to the underlying Au substrates. Surprisingly, the AuNPs were found to aggregate during their immobilization to different extents depending on the substrate roughness. Transmission electron microscopy (TEM), atomic force microscopy (AFM), and UV–vis spectrophotometry were used to probe the aggregation phenomena of AuNPs in the solution phase (i.e., before immobilization) and after being anchored on the different Au substrates. The extent of AuNPs' aggregation is inversely proportional to the Au substrate roughness (which is directly related to the surface coverage of the self-assembled monolayer (SAM) of the BDMT binder). AuNPs with average particle size of 4.0, 5.5 and 8.0 nm were obtained upon the immobilization onto Au substrates with roughness factor of 3.07, 2.49 and 1.1, respectively.

Keywords: Gold nanoparticles; TEM; AFM; Layer-by-layer; Surface roughness; Aggregation

1. Introduction

Nanoscale materials attract continuously growing interests due to their unprecedented fascinating properties over their corresponding bulk materials, such as the high effective surface area, catalytic activity, quantum confinement, etc. [1–6]. The stimulus for this growth can be traced to new and improved approaches of making and assembling, positioning and connecting, imaging and measuring the properties of nanomaterials with controlled size and shape, composition and surface structure, charge and functionality, for use in the macroscopic real world [7]. Gold nanoparticles (AuNPs) are extensively studied in view of their potential applications in electronics, optoelectronics, as well as chemical and electrochemical catalysis [4,8,9]. The layer-by-layer (LBL) technique, among the anchoring techniques, is a facile and flexible procedure used for the preparation of super-structured nanoparticles arrays [10–15].

We have recently reported on the LBL-based fabrication of three-dimensional alternative multilayer arrays of citrate-stabilized gold nanoparticles on gold substrate [16,17]. 1,4-Benzenedimethanethiol (BDMT) was used as a cross-linker to connect the nanoparticles together in a three-dimensional network. Surprisingly, a two to three times increase of the average particle size of the anchored AuNPs has been observed [18]. This revealed the occurrence of aggregation during the nanoparticles' immobilization on the BDMT layer. The catalytic activity of AuNPs is inherently related to their particle size, and this urged us to investigate the reason behind the observed aggregation and possibly to control its extent. This would enable the fabrication of anchored AuNPs with tunable size suitable for a desired application. In solution phase, several groups have addressed, controlled and sometimes utilized the AuNPs' aggregation phenomenon [9,19–22]. Basically, a group of stabilizers including low molecular weight surfactants, organic thiols, thiol-functionalized ionic liquid, inorganic ligands and various

* Corresponding author. Tel.: +81 45 924 5404; fax: +81 45 924 5489.
E-mail address: ohsaka@echem.titech.ac.jp (T. Ohsaka).

0927-7757/$ – see front matter © 2008 Published by Elsevier B.V.
doi:10.1016/j.colsurfa.2007.12.013

polymeric materials have been used to isolate the AuNPs and prevent their aggregation in the solution phase [9,18,19,23]. The molar ratio of Au atoms to the stabilizer is a crucial parameter which determines the final average size of the AuNPs [23]. In some cases, citric acid was used as a photochemical reducing agent of the Au ions which act as a stabilizer for the prepared AuNps as well [24]. In that case, the pH of the medium also contributes in defining average size of AuNPs [24]. In ethanolic solution, Liao et al. [20] have observed a spontaneous linear aggregation of AuNPs and the dipole–dipole interaction was believed the driving force for this aggregation. On the other hand, a reversible aggregation/deaggregation process of the AuNPs has been achieved in a dithiol-containing solution [19].

So far, little information is available regarding the aggregation of AuNPs during their immobilization onto solid substrates. The aim of this work is to investigate and possibly to control the aggregation of AuNPs immobilized on gold substrates using BDMT as a cross-linker. Three Au substrates with different roughness factor (r.f. = real area/geometric area) were employed in this study. The results showed a dependency of the extent aggregation on the substrate morphology (i.e., roughness). The aggregation phenomena of AuNPs in solutions containing BDMT or cystamine is also addressed and interpreted.

2. Experimental

2.1. Electrodes preparation and pretreatment

Three Au substrates were utilized, namely, polycrystalline gold (poly-Au), poly-Au with electrochemically (EC) deposited gold nanoparticles (EC-poly-Au), and atomically flat Au(1 1 1) single crystal electrodes. The Au(1 1 1) electrode was softly cleaned by successive sonication in acetone, ethanol, and deionized water. Conventional procedures were applied to clean the poly-Au electrodes ($\phi = 1.6$ mm). Typically, the electrodes were mechanically polished with emery paper (2000-grade), then with aqueous slurries of successively finer alumina powder (particle size down to 0.06 μm) with the help of a polishing microcloth. The poly-Au electrodes were, then, electrochemically cleaned by cycling the potential between −0.2 and 1.5 V vs. Ag | AgCl in N_2 saturated 0.5 M H_2SO_4 at scan rate of 10 V s^{-1} for 10 min or until the cyclic voltammogram characteristic of a clean Au surface is obtained. The EC-poly-Au electrode was prepared by depositing AuNPs electrochemically onto the poly-Au electrode by applying a potential step electrolysis from 1.1 to 0.0 V vs. Ag | AgCl for 60 s in an acidic aqueous solution of 0.5 M H_2SO_4 containing 1.0 mM $Na[AuCl_4]$ and 100 μM I^- ions. Thus, AuNPs of average particle size of about 10–20 nm were electrodeposited onto the poly-Au electrodes (denoted hereafter as EC-poly-Au) [25–27]. Then, the EC-poly-Au electrode was cleaned electrochemically to remove the adsorbed iodide ions. The real surface area of the different Au substrates was estimated by calculating the charge consumed during the reduction of the Au surface oxide monolayer (formed during the anodic scan) in N_2-saturated 0.5 M H_2SO_4 solution (peak located at ca. +900 mV vs. Ag | AgCl [28]) using a reported value of 400 μC cm^{-2} [28]. The roughness factor (r.f.) was estimated accordingly for each electrode (cf. Table 1).

2.2. Chemical immobilization of the AuNPs

Chemicals of analytical grade were used in this study. The chemical immobilization of the AuNPs onto the three different Au substrates has been performed in three consecutive steps. Firstly, a colloidal solution of citrate-stabilized AuNPs (average particle size = 2.3 nm) was chemically prepared according to a well-established procedure [18]. Typically, 1 ml of 1% $NaAuCl_4$ (Wako, Japan) was added to 90 ml of water at room temperature (25 ± 1 °C) and the solution was stirred for 1 min. Subsequently, 2 ml of 38.8 mM sodium citrate followed by another 1 ml of freshly prepared 0.075 wt% $NaBH_4$ in 38.8 mM sodium citrate were dropwise added and the colloidal solution was left under stirring for about 10 min. The thus-prepared colloidal AuNPs solution is, then, stored in a dark bottle at 4 °C. Secondly, a dithiol binder (i.e., with two terminal thiol groups) is self-assembled onto the Au substrates. BDMT molecule is a typical binder which forms a self-assembled monolayer (SAM) onto the surface of gold electrodes (through the formation of a covalent Au–S bond with the loss of one thiol proton). The other free thiol group of the BDMT molecule (facing the solution side) has a strong tendency to anchor the AuNPs through the formation of Au–S covalent bond [29]. Thus, a monolayer of BDMT has been self-assembled onto the different Au substrates by soaking the clean Au electrodes into an ethanolic solution of 1.0 mM BDMT (Aldrich) for 1 h. The surface coverage of the BDMT monolayer (Γ_{BDMT}) is found to depend on the morphology (i.e., surface roughness) of the underlying Au substrate (cf. Table 1). Lastly, the as-prepared BDMT-SAM-modified Au electrodes were subsequently washed well with copious amount of ethanol and water, and then immersed in the citrate-stabilized AuNPs colloidal solution for 12 h at room temperature to allow for the immobilization of the AuNPs atop of the BDMT monolayer. The electrodes were, then, rinsed well with water and moved to measurements.

Table 1
The dependency of the average size of AuNPs immobilized on BDMT-modified gold substrates on the substrate roughness and the BDMT' surface coverage

Substrate	Roughness factor	Γ_{BDMT} ($\times 10^9$ mol cm^{-2})[a]	Average size of AuNPs (nm)
Au(1 1 1)	1.10	0.914	8.2
Poly-Au	2.49	2.145	5.5
EC-poly-Au	3.07	2.558	4.0

[a] The surface coverage is normalized based on the geometric surface area.

2.3. Characterization of the AuNPs

Transmission electron microscopic (TEM) images were captured using a JEM-2010F analytical microscope operated at an acceleration voltage of 200 kV with a resolution of 0.1 nm and a magnification factor (×) of 50–1,500,000. Atomic force microscopic (AFM) image was obtained *ex situ* using an AFM Nanoscale Hybrid Microscope VN-8000-KEYENCE, in the direct contact mode. The UV–vis spectra of the different thiol-containing AuNPs colloidal solutions were obtained using a Hitachi spectrophotometer (Hitachi U-3300 with 10-mm length quartz cell).

3. Results and discussion

The UV–vis spectral analysis of the citrate-stabilized colloidal solution of the AuNPs has been frequently utilized to probe their average particle size. The appearance of a peak at ca. 516 nm (cf. Fig. 2A) reflects the formation of AuNPs with an average size of 2.3 nm [30–32], in agreement with the observation of previous report [18]. And this, of course, does not deny the formation of a very small amount (i.e., undetectable under the present experimental conditions) of bigger AuNPs. It is believed that a negatively charged citrate sphere is surrounding the individual AuNPs in the colloidal solution inducing a repulsive interaction between the nanoparticles and, thus, stabilizes the AuNPs and reduces their aggregation. Fig. 1 shows a typical TEM image of AuNPs monolayer immobilized on poly-Au electrode with the assistance of BDMT as a binder. Investigation of this image revealed an average particle size of around 5.5 nm for the anchored AuNPs monolayer. This value is a little larger than twice that of the chemically prepared AuNPs in the citrate-stabilized colloidal solution. This inferred that a few AuNPs aggregated during the anchoring process. The

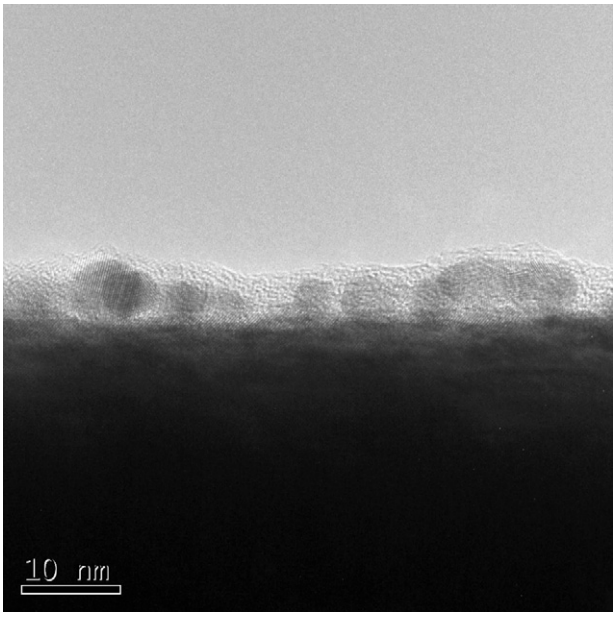

Fig. 1. TEM image for chemically anchored AuNPs immobilized over polycrystalline gold substrate.

aggregation phenomena of AuNPs have been addressed in the solution phase [9,18,19]. However, to the best of our knowledge, the aggregation control of AuNPs during their immobilization onto solid substrates is not yet addressed. Several factors are believed to influence the extent of AuNPs aggregation during their anchoring on gold electrodes. Some of these factors are related to the substrate itself and others are related to the binder and/or stabilizer. In a trial to explore the origin of the aggregation phenomenon of the AuNPs during their immobilization, the following points should be stressed. The anchoring of the AuNPs by the BDMT monolayer occurs due to the formation of –S–Au covalent bond between the terminal –SH group (of the BDMT) and the AuNPs (in the solution phase). This necessitates an instantaneous uncovering of the physically adsorbed citrate sphere away from the AuNPs. Thus, a physical–chemical model might furnish a plausible explanation of the replacement of the citrate sphere (away from the surface of the AuNPs) with the thiol covalent bond formation.

The extent of the removal of the citrate sphere (i.e., deshielding of the AuNPs) is a crucial parameter that likely depends on the surface concentration of the BDMT monolayer (Γ_{BDMT}) and thus controls the extent of AuNPs aggregation. To confirm this, we have examined the effect of the binder concentration on the extent of aggregation of citrate-stabilized AuNPs in the solution phase. Various amounts of BDMT (in the μM range) were added to a constant volume of the citrate-stabilized AuNPs colloidal solution. Surprisingly, an immediate precipitation of the AuNPs was always observed independent of the amount of BDMT added. This indicated that a high degree of aggregation occurred in the AuNPs colloidal solution. In this case, BDMT acted as a powerful cross-linking agent as it has two active terminal thiol (–SH) groups. In the solution phase, the two thiol groups (attached to one BDMT molecule) are able to induce the removal of the citrate sphere away from the surface of the colloidal AuNPs and thus to bond covalently with the AuNPs in all dimensions. In view of the relative dimensions, one should also realize that one Au nanoparticle can bond to more than one BDMT molecule, and each BDMT molecule can connect two AuNPs. Therefore, a high molecular weight cross-linked BDMT-AuNPs 3D network is formed and precipitated. It is worth mentioning here that such huge aggregation did not occur when AuNPs were anchored on BDMT-modified poly-Au electrodes since only one thiol group of the BDMT molecule is freely allowed to interact with AuNPs. Whereas, the other –SH group of the BDMT is being consumed to covalently immobilize the BDMT molecules on the surface of the poly-Au electrode. The binder-induced aggregation in the solution phase was further investigated using another thiol (binder) compound with lower cross-linking ability, typically cystamine ($HS–CH_2–CH_2–NH_2$). It has two terminal functional groups; one is the mercapto (–SH) group and the other is the amine ($–NH_2$) group. The –SH group and the positively charged amino groups bond covalently and electrostatically, respectively, to the citrate-stabilized AuNPs [16,17]. Thus, the uncovering of the citrate sphere is less predominant. And consequently, the probability of aggregation and the formation of the 3D network decreases in the solution phase. That was verified by the addition

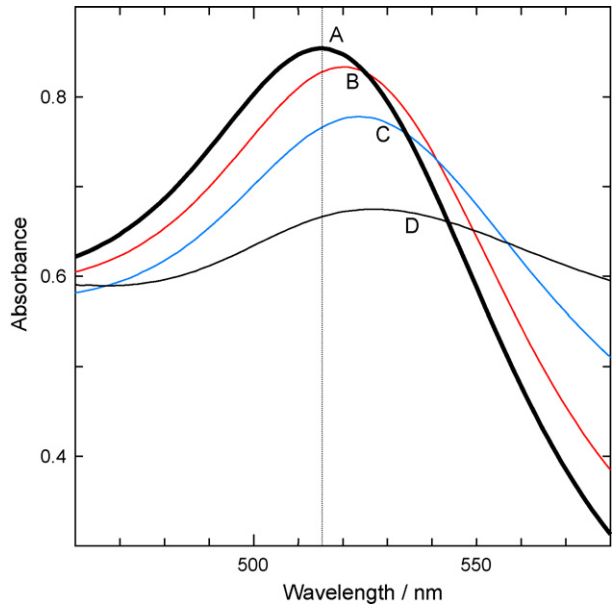

Fig. 2. UV–vis absorption spectra of AuNPs' colloidal solutions containing (A) 0 μM, (B) 2 μM, (C) 10 μM, and (D) 20 μM cystamine.

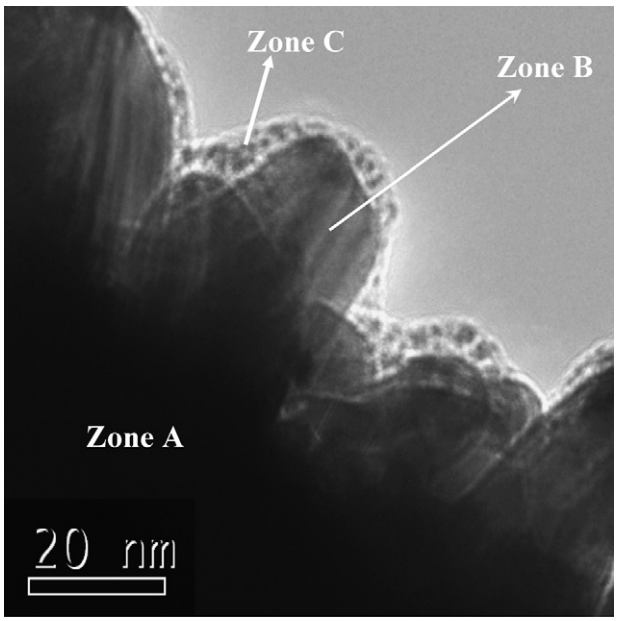

Fig. 3. TEM image for the AuNPs chemically immobilized on EC-poly Au substrate. Zones A, B and C are, respectively, for poly-Au substrate, electrochemically deposited Au nanoparticles, and the chemically anchored AuNPs.

of different amounts of cystamine (in the μM range) to a colloidal solution of citrate-stabilized AuNPs. Fig. 2 represents the UV–vis absorption spectra of various AuNPs solutions after the addition of different concentrations of cystamine. The spectrum of a blank AuNPs colloidal solution (cystamine-free, curve A) has an optical absorption peak at 516 nm arisen from the surface plasmon resonance [30–32]. Curves B, C, and D of Fig. 2 show, respectively, the spectra of AuNPs colloidal solutions after the addition of 2, 10, and 20 μM of cystamine. A gradual red shift accompanied by a peak broadening was observed upon the increase of the cystamine concentration, concurrently, with a change in the colloidal AuNPs solution from red to purple. The red shift and the color change are together a direct evidence for the particle size increase [33]. Higher concentrations of cystamine (>20 μM) resulted in a precipitation of AuNPs similarly to BDMT. Therefore, it can be concluded that the origin of aggregation during immobilization of AuNPs on poly-Au electrode is the instantaneous binder-induced removal of the citrate sphere away from the surface of the AuNPs. During that short time of de-shielding, several AuNPs aggregate to decrease their overall surface energy.

The effect of the substrate roughness (i.e., microtopography) has been further investigated using smooth Au(1 1 1) and rough EC-poly-Au electrodes. The EC-poly-Au electrode was made by electrodepositing AuNPs form an acidic bath containing 1.0 mM $Na[AuCl_4]$ and 100 μM I^- ions. The particle size distribution of the electrodeposited AuNPs was ca. 10–20 nm [25–27]. The electrodeposition of AuNPs on poly-Au substrate was done to increase the roughness of the electrode. The roughness factors (r.f.) of the EC-poly-Au and Au(1 1 1) electrodes were, respectively, 3.07 [34], and 1.1 [35], whereas the r.f. of the poly-Au electrode was 2.49. The TEM image shown in Fig. 3 illustrates the morphology of the AuNPs after their immobilization onto the EC-poly-Au substrate. Interestingly, a smaller average size (4.0 nm) was obtained for the anchored AuNPs (zone C). This means that the aggregation of the AuNPs occurred to a lesser extent than that observed on the poly-Au electrode (see Fig. 1). Immobilization of AuNPs was next performed on a single crystalline Au(1 1 1) substrate and the sample was pictured by AFM. Fig. 4 displays a three-dimensional AFM image for the Au(1 1 1) substrate after the chemical immobilization of a monolayer of AuNPs using the BDMT binder. Investigation of the surface profile of this sample revealed a thickness of 8.2 nm for the AuNPs layer, i.e., a higher extent of aggregation occurred on the Au(1 1 1) than that on poly-Au substrate. These results point out that the decrease of the Au substrate roughness leads to a higher extent of aggregation of the anchored AuNPs.

In fact, the change of the Au substrate roughness is associated with a change of the surface concentration of the BDMT-SAM binder (i.e., Γ_{BDMT}) which might affect the extent of aggre-

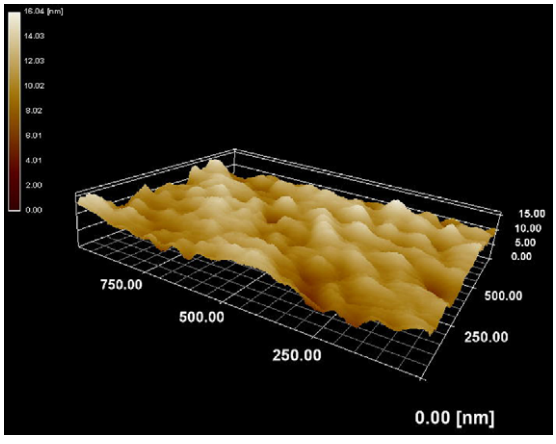

Fig. 4. Three-dimensional AFM image for AuNPs immobilized on Au(1 1 1) single facet substrate.

gation of the anchored AuNPs. To estimate the BDMT surface coverage (Γ_{BDMT}), the reductive desorption patterns of a full monolayer of BDMT-SAM (formed at the three different Au substrates) have been measured in N_2-saturated 0.5 M KOH solution and the results are shown in Fig. 5. The surface of poly-Au electrode is considered to compose, mainly, of three low-index crystallographic orientations (Au(1 1 1), Au(1 0 0), and Au(1 1 0)) with a huge number of kinks and steps [36]. Each single-crystalline domain exhibits a different binding strength toward the self-assembled thiol, which results in the appearance of multiple desorption peaks. However, in the case of BDMT-SAM, broad peak accompanied by a small shoulder appeared in the reductive desorption pattern of the three different substrates (see Fig. 5, curve a). Another interesting point is the existence of a negative shift of about 40 mV in the desorption peak in the case of BDMT-SAM-modified EC-poly-Au substrate (curve b) and a positive shift of about 240 mV for that of the BDMT-SAM-modified Au(1 1 1) substrate (curve c) in comparison to that of BDMT-SAM-modified poly-Au substrate (curve a). The lateral interaction among the hydrophobic BDMT molecules is likely the reason preventing the appearance of a sequentially separated desorption pattern similar to the case of a short chain thiol-SAM (e.g., cysteine) [36]. Integration of the faradaic charge associated with reductive desorption of the BDMT-SAM is used to estimate Γ_{BDMT}. The values of Γ_{BDMT} for the three Au electrodes are listed in Table 1. This table shows that Γ_{BDMT} increases with increasing the substrate roughness which is associated with a decrease of the average particle size of the subsequently anchored AuNPs. A high surface coverage of BDMT reduces their aggregation by efficiently binding them to the surface. This means that a high surface coverage of BDMT molecules is required to reduce the aggregation and stabilize the anchored AuNPs. On the other hand, at low Γ_{BDMT}, the probability of nanoparticle–nanoparticle interaction increases to relief the excess surface energy and consequently the extent of aggregation increases. The scheme in Fig. 6 illustrates the immobilization of AuNPs on two different substrates (smooth and rough). It shows clearly that the BDMT surface coverage is critical to control the extent of aggregation.

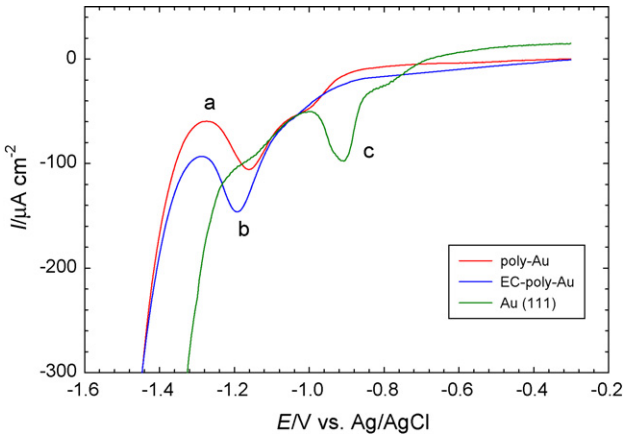

Fig. 5. Linear scan voltammetry for the reductive desorption of BDMT assembled on (a) poly-Au, (b) EC-poly-Au, (c) single crystalline Au(1 1 1) substrates measured in 0.5 M KOH solution (scan rate 50 mV s^{-1}).

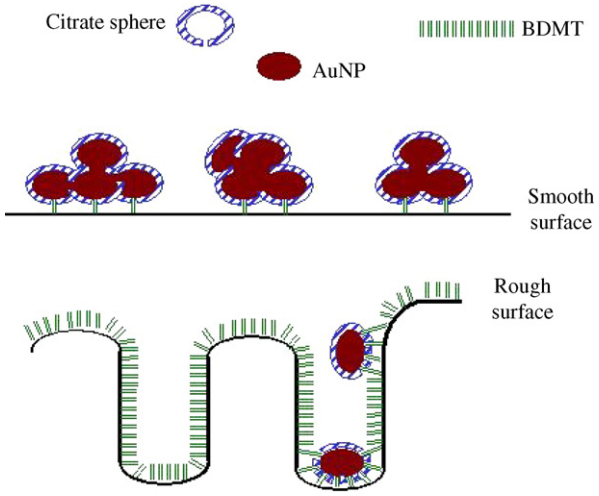

Fig. 6. A schematic representing the effect of the BDMT surface coverage on the extent of AuNPs' aggregation.

It has been previously thought that nanoparticles preserve their morphology when immobilized from solutions to substrates, and therefore the anchored AuNPs would retain their morphology similar to that in the solution phase before anchoring [20]. Our results showed that it is not always true, and in some cases a morphological change (e.g., aggregation) of nanoparticles may occur upon immobilization. The use of rougher/smoother Au substrates and employing AuNPs with different average particles size are currently under way.

4. Conclusions

This study is concerned with the investigation of the aggregation phenomena of the chemically prepared citrate-stabilized AuNPs during their immobilization onto Au substrates with different surface roughness. A monolayer of BDMT was self-assembled on the electrodes and was, then, used as an anchoring agent for the AuNPs. The immobilization process of the AuNPs necessitates the uncovering of the AuNPs (i.e., removal of the citrate sphere away from the AuNPs) to allow for the –S–Au covalent bond formation. The extent of the instantaneous uncovering of the citrate shield depended on the surface concentration of the thiol binder (which was, in turn, related to the roughness of the underlying Au substrate). That is, AuNPs of an average size of about 8.2 nm are formed at a smooth Au substrate (Au(1 1 1), r.f. = 1.1), whereas, AuNPs of smaller average size (about 4.0 nm) were anchored onto a relatively rough substrate (EC-poly-Au, r.f. = 3.07).

Acknowledgments

The present work was financially supported by Grant-in-Aids for Scientific Research on Priority Areas (No. 417), Scientific Research (No. 12875164) and Scientific Research (A) (No. 19206079) to T. Ohsaka, from the Ministry of Education, Culture, Sports, Science and Technology (MEXT), Japan and also by New Energy and Industrial Technology Development Organization (NEDO), Japan and also by Japan-China Joint Research

Program on "Science and Technology for Environmental Conservation and Construction of a Society with Less Environmental Burden", organized and sponsored by Japan Science and Technology (JST) and National Natural Science Foundation of China (NSFC). Authors acknowledge Dr. A. Genski at Center for Advanced Materials Analysis of Tokyo Institute of Technology and Mr. H. Masmitsu at R&D group of Keyence Co., Japan for their assistance in the TEM and AFM measurements, respectively. A.I.A. acknowledges a MEXT scholarship from the Japanese Government. M.S. El-Deab thanks the Japan Society for the Promotion of Science (JSPS) for the Invitation fellowship.

References

[1] A.P. Alivisatos, Science 271 (1996) 933–937.
[2] A.P. Alivisatos, K.P. Johnsson, X. Peng, T.E. Wilson, C.J. Loweth, M.P. Bruchez Jr., P.G. Schultz, Nature 382 (1996) 609–611.
[3] D.G. Schultz, X.-M. Lin, D. Li, J. Gebhardt, M. Meron, J. Viccaro, B. Lin, J. Phys. Chem. B 110 (2006) 24522–24529.
[4] M.-C. Daniel, D. Astruc, Chem. Rev. 104 (2004) 293–346.
[5] R. Zanella, A. Sandoval, P. Santiago, V.A. Basiuk, J.M. Saniger, J. Phys. Chem. B 110 (2006) 8559–8565.
[6] C.F. Vardeman, P.F. Conforti, M.M. Sprague, J.D. Gezelter, J. Phys. Chem. B 109 (2005) 16695–16699.
[7] G. Ozin, A. Arsenault, Nanochemistry: A Chemistry Approach to Nanomaterials, Springer Verlag, New York, 2005.
[8] M.S. El-Deab, T. Ohsaka, Electrochem. Commun. 4 (2002) 288–292.
[9] J.H. Youk, M.-K. Park, J. Locklin, R. Advincula, J. Yang, J. Mays, Langmuir 18 (2002) 2455–2458.
[10] H.-L. Zhang, S.D. Evans, J.R. Henderson, Adv. Mater. 15 (2003) 531–534.
[11] C. Jiang, S. Markutsya, V.V. Tsukruk, Langmuir 20 (2004) 882–890.
[12] X. Zhou, C. Liu, Z. Zhang, L. Jiang, J. Li, J. Colloid Interface Sci. 284 (2005) 354–357.
[13] H. Zhang, H. Lu, N. Hu, J. Phys. Chem. B 110 (2006) 2171–2179.
[14] L. Gao, E. Wang, Z. Kang, Y. Song, B. Mao, L. Xu, J. Phys. Chem. B 109 (2005) 16587–16592.
[15] F.N. Crespilho, M. Emilia Ghica, M. Florescu, F.C. Nart, O.N. Oliveira Jr., C.M.A. Brett, Electrochem. Commun. 8 (2006) 1665–1670.
[16] A.I. Abdelrahman, A.M. Mohammad, T. Okajima, T. Ohsaka, J. Phys. Chem. B 110 (2006) 2798–2803.
[17] C.R. Raj, A.I. Abdelrahman, T. Ohsaka, Electrochem. Commun. 7 (2005) 888–893.
[18] K.R. Brown, D.G. Walter, M.J. Natan, Chem. Mater. 12 (2000) 306–313.
[19] C. Guarise, L. Pasquato, P. Scrimin, Langmuir 21 (2005) 5537–5541.
[20] J. Liao, Y. Zhang, W. Yu, L. Xu, C. Ge, J. Liu, N. Gu, Colloid Surf. A 223 (2003) 177–183.
[21] M. Brust, C.J. Kiely, D. Bethell, D.J. Schiffrin, J. Am. Chem. Soc. 120 (1998) 12367–12368.
[22] Y. Yang, S. Matsubara, M. Nogami, J. Shi, Mater. Sci. Eng. B 140 (2007) 172–176.
[23] Y. Jin, P. Wang, D. Yin, J. Liu, L. Qin, N. Yu, G. Xie, B. Li, Colloid Surf. A 302 (2007) 366–370.
[24] S. Yang, Y. Wang, Q. Wang, R. Zhang, B. Ding, Colloid Surf. A 301 (2007) 174–183.
[25] M.S. El-Deab, T. Sotomura, T. Ohsaka, Electrochem. Commun. 7 (2005) 29–34.
[26] M.S. El-Deab, T. Sotomura, T. Ohsaka, J. Electrochem. Soc. 152 (2005) C730.
[27] M.S. El-Deab, T. Sotomura, T. Ohsaka, J. Electrochem. Soc. 152 (2005) C1.
[28] S.P. Trasatti, O.A. Petrii, Pure Appl. Chem. 63 (1991) 711–734.
[29] K.V.G.K. Murty, M. Venkataramanan, T. Pradeep, Langmuir 14 (1998) 5446–5456.
[30] A. Taleb, C. Petit, M.P. Pileni, J. Phys. Chem. B 102 (1998) 2214–2220.
[31] A. Henglein, Langmuir 15 (1999) 6738–6744.
[32] C.F. Bohren, D.R. Huffman, Absorption and Scattering of Light by Small Particles, John Wiley & Sons, New York, 1983.
[33] K. Sato, K. Hosokawa, M. Maeda, J. Am. Chem. Soc. 125 (2003) 8102–8103.
[34] M.S. El-Deab, T. Ohsaka, Electrochim. Acta 47 (2002) 4255–4261.
[35] S.-S. Wong, M.D. Porter, J. Electroanal. Chem. 485 (2000) 135–143.
[36] K. Arihara, T. Ariga, N. Takashima, K. Arihara, T. Okajima, F. Kitamura, K. Tokuda, T. Ohsaka, Phys. Chem. Chem. Phys. 5 (2003) 3758–3761.